

Environmental effects on the bright end of the galaxy luminosity function in galaxy clusters

R. Barrena^{1,2}, M. Girardi^{3,4}, W. Boschin⁵, and F. Mardirossian^{3,4}

¹ Instituto de Astrofísica de Canarias, C/Vía Láctea s/n, E-38205 La Laguna (Tenerife), Canary Islands, Spain

² Departamento de Astrofísica, Universidad de La Laguna, Av. del Astrofísico Francisco Sánchez s/n, E-38205 La Laguna (Tenerife), Canary Islands, Spain

³ Dipartimento di Fisica dell' Università degli Studi di Trieste - Sezione di Astronomia, via Tiepolo 11, I-34143 Trieste, Italy

⁴ INAF - Osservatorio Astronomico di Trieste, via Tiepolo 11, I-34143 Trieste, Italy

⁵ Fundación Galileo Galilei - INAF, Rambla José Ana Fernández Perez 7, E-38712 Breña Baja (La Palma), Canary Islands, Spain

Received / Accepted

ABSTRACT

Context. The dependence of the luminosity function (LF) of cluster galaxies on the evolutionary state of the parent cluster is still an open issue, in particular as concern the formation/evolution of the brightest cluster galaxies.

Aims. We plan to study the bright part of the LFs of a sample of very unrelaxed clusters (“DARC” clusters showing evidence of major, recent mergers) and compare them to a reference sample of relaxed clusters spanning a comparable mass and redshift range.

Methods. Our analysis is based on the SDSS DR7 photometric data of ten, massive, and X-ray luminous clusters ($0.2 \lesssim z \lesssim 0.3$), always considering physical radii (R_{200} or its fractions). We consider r' band LFs and use the color-magnitude diagrams ($r' - i', r'$) to clean our samples as well to consider separately red and blue galaxies.

Results. We find that DARC and relaxed clusters give similar LF parameters and blue fractions. The two samples differ for their content of bright galaxies BGs, $M_r < -22.5$, since relaxed clusters have fewer BGs, in particular when considering the outer cluster region $0.5R_{200} < R < R_{200}$ (by a factor two). However, the cumulative light in BGs is similar for relaxed and DARC samples.

Conclusions. We conclude that BGs grow in luminosity and decrease in number as the parent clusters grow hierarchically in agreement with the BG formation by merging with other luminous galaxies.

Key words. Galaxies: clusters: general – Galaxies: luminosity functions – Cosmology: observations

1. Introduction

The study of the formation and evolution of galaxies is a fundamental avenue of research in the process of understanding astrophysical and cosmological issues. The galaxy luminosity function (LF) – the number of galaxies per unit volume in the luminosity interval L and $L + dL$ – is one of the most direct observational test of theories of galaxy formation and evolution.

Clusters of galaxies are ideal systems within which to measure the galaxy LF for the large number of galaxies at the same distance. On the other hand, clusters represent an extreme environment for galaxy evolution, either in situ or through the accretion of galaxies within groups, which are situated in the filamentary structure of the hierarchical Universe (e.g., Poggianti et al. 2005).

While introducing the modern form of the LF, the so-called “Schechter Function”, Schechter (1976) suggested that the cluster LF is universal in shape (with a turnover at $M_B^* = -20.6 + 5 \log h_{50}$ and a faint-end slope of $\alpha = -1.25$). Much progress has then been made in looking for possible observational signatures of a non universality of the cluster LF. That different morphological types are characterized by different LFs (Binggeli et al. 1988) and the well known morphological segregation with the

local density and thus the clustercentric radius (Dressler 1978; Whitmore 1991) make more complex the study of the cluster LF. In this context, several studies about LF concern the possible variation of the cluster LF with the local projected galaxy density and/or cluster-centric radius. In particular, there are claims for a radius-dependent steepening of the galaxy LF at faint magnitudes, likely due to red galaxies (e.g., de Propris 1995; Driver et al. 1998; Popesso et al. 2006; Barkhouse et al. 2007). However, the few cases of LFs based on deep spectroscopy exhibit shallower slopes (e.g., Rines & Geller 2008 and refs. therein) suggesting that the field contamination might be the cause of the observed steep LFs based on photometry only. Thus, the question is still far from a definitive conclusion.

Another issue concerns the possible dependence of the LF on global cluster properties. Some studies interest a few well studied clusters and/or cluster complexes (e.g., Abell 209 in Mercurio et al. 1996, Coma vs. Abell 1367 in Iglesias-Páramo et al. 2003) and other studies use instead a large statistical base. In particular, there are indications in favour of correlations between the LF parameters and the cluster mass or its proxies (e.g., richness, luminosity, galaxy velocity dispersion). For instance, Valotto et al. (1997) find that poorer clusters have a flatter LF. But, when the LF is properly calculated within the cluster physical sizes, given by R_{200} or R_{500} , the correlation between the

Send offprint requests to: R. Barrena, e-mail: rbarrena@iac.es

dwarf-to-giant ratio and X-ray (or optical) luminosity disappear (cf. Popesso et al. 2006 with Popesso et al. 2004). This suggests that the radial behavior of the LF should be taken into account to obtain unbiased conclusions. However, also when considering an appropriate cluster physical size, the conclusions are not all consistent. For example, Hilton et al. (2005) find that clusters with lower X-ray luminosity have a brighter M^* , but Barkhouse et al. (2007) find no correlation. Recent studies also attempt to analyze more distant clusters, but again with no conclusive results (Gilbank et al. 2008; Rudnick et al. 2009 and discussion therein).

Possible correlations with the presence/absence of a cD galaxy or with the Bautz-Morgan type (the BM-type classification based on the brightest cluster galaxies, BCGs, Bautz & Morgan 1970), are, maybe, also more interesting for their direct connection with the cluster evolutionary state. In fact, BCGs or cD galaxies are expected to be created i) via the merger of giant galaxies in an early phase during the cluster collapse (Merritt 1984) or ii) in a following phase due to the dynamical friction acting on late-comer galaxies (e.g., Ostriker & Tremaine 1975) or iii) via the disruption and cannibalization of many faint galaxies in the cluster cores (López-Cruz et al. 1997). The first two mechanisms might reduce the number of bright galaxies, thus shifting M^* to a fainter value and, indeed, Barkhouse et al. (2007) find a weak correlation with the BM-type (but see de Propriis et al. 2003 for no correlation). Another consequence can be the increment of the gap between the first and the second brightest galaxies in each cluster and, in fact, this magnitude gap is shown to be larger in clusters without substructure and smaller in clusters with substructure (Ramella et al. 2007).

As for the second mechanism, López-Cruz et al. (1997) find that seven rich, massive, cD clusters with symmetric X-ray morphology show a flat faint-end slope while a steeper faint-end slope is detected in poorer clusters but also in a rich, binary cluster like the Coma cluster. Somewhat in agreement, Driver et al. (1998) find that the dwarf-to-giant ratio increases with larger BM-types (i.e., likely less evolved clusters). In this context, Valotto et al. (2004) pointed out the importance of the projection effects in determining the faint-end slope. In fact, in the large cluster sample analyzed by Valotto et al. it is the X-ray selection and not the cluster domination by central galaxies what determines the flatness of the faint-end slope thus suggesting that real, compact clusters are less affected by the field contamination. However, although this bias could explain possible differences between rich and poor clusters, the reason for the difference between the seven cD relaxed clusters of López-Cruz et al. (1997) and the Coma cluster is not clear yet.

As for the possible dependence of the LF on the dynamical status of the cluster, the noticeable study of de Propriis et al. (2003) analyze 60 clusters and find that the LF is similar for clusters with and without substructure. Very few detailed works are devoted to study the LFs of subclumps in individual clusters to find possible evidence of cluster mergers (e.g., Durret et al. 2011).

As reported above, it is particularly interesting the bright end of the LF since there is a long debate on the BCG formation. For instance, semianalytical models suggest that BCGs assemble surprisingly late with the stars formed very early in many small galaxies (e.g., 50% at $z=0.5$, 80% at $z=0.3$; see de Lucia & Blaizot 2007). However, photometric and chemical observables suggest that it is difficult to explain giant elliptical by a pure sequence of multiple minor dry mergers or via major dry mergers (e.g., Stott et al. 2010; Ascaso et al. 2011) and numerical simulations are continuously improved to reproduce them

better (e.g., Ruszkowski & Springel 2009). Moreover, galaxy-galaxy mergers are most efficient within small halos with small velocity dispersion and the merger of BCGs in clusters requires a long time (Dubinski 1998). However, the correlation between BCG luminosity and parent cluster mass strongly suggest that BCGs co-evolves with the cluster (Lin & Mohr 2004).

In this context, we plan to study the LFs of a sample of massive and very unrelaxed clusters and compare them to a reference sample of relaxed clusters spanning a comparable mass and redshift range.

As for the unrelaxed clusters, we are going on with a long term project to study clusters exhibiting large, diffuse radio sources, i.e. radio halos and relics, based on spectroscopic data mostly acquired at TNG (DARC - Dynamical Analysis of Radio Clusters¹ - e.g., Girardi et al. 2007). These radio sources are rare phenomena and are due to the synchrotron radio emission of widespread relativistic particles embedded in the cluster magnetic field (e.g., see Feretti et al. 2002b for a review). Cluster mergers have been proposed to provide the large amount of energy necessary for electron reacceleration to relativistic energies and for magnetic field amplification (e.g., Tribble 1993; Ensslin et al. 1998; Brunetti et al. 2009) or required to explain the time-dependence of the magnetic fields in recent models based on secondary electrons (Keshet & Loeb 2010; Keshet 2011). Indeed, from the observational point of view, there is growing evidence of the connection between diffuse radio emission and cluster merging, since up to now diffuse radio sources have been detected only in merging systems. In most past studies the cluster dynamical state was derived from X-ray observations (see Buote 2002; Feretti 2006 and 2008; Cassano et al. 2010). In agreement, our analyses, based on optical data and the kinematics of member galaxies, detect strong subclustering and find evidence of cluster mergers. Summarizing, clusters with radio halos/relics are the ideal cases to study the effect of the cluster formation on the LF.

Here we analyze a subsample of five DARC clusters we have analyzed in the past and all having available photometry in the Sloan Digital Sky Survey (SDSS). The DARC clusters form our sample of unrelaxed clusters. For comparison, we analyze a sample of relaxed clusters of comparable mass and redshift. Considering the magnitude limit of SDSS photometry, the typical redshift of the samples, $z \sim 0.25$, limits our study to the bright part of the LF. We plan to extend this study to a fainter magnitudes in the next future.

Unless otherwise stated, we give errors at the 68% confidence level (hereafter c.l.).

Throughout this paper, we use $H_0 = 70 \text{ km s}^{-1} \text{ Mpc}^{-1}$ in a flat cosmology with $\Omega_0 = 0.3$ and $\Omega_\Lambda = 0.7$. We define $h_{70} = H_0/(70 \text{ km s}^{-1} \text{ Mpc}^{-1})$.

2. Cluster sample

Among the DARC clusters of which we have already analyzed the internal dynamics using a large number of member galaxies, five clusters (with 62-113 spectroscopic member galaxies) have also available photometry in the SDSS (Data Release 7): Abell 697, Abell 773, Abell 959, Abell 1240, and Abell 2219, hereafter A697, A773, A959, A1240, A2219 (see Table 1 for the respective reference sources). Their redshifts span the range $z = 0.19 - 0.29$ and they are characterized by high line-of-sight galaxy (LOS) velocity dispersion σ_v , X-ray temperature T_X , and

¹ other information are given in the web site <http://adlibitum.oat.ts.astro.it/girardi/darc>.

mass M (see Table 1). Evidence for their unrelaxed dynamical state is reported in our previous studies. In particular, they span different angle of views for the merging axis. For instance, the cluster merger occurred largely in the plane of the sky in A1240 and largely along the LOS in A773.

As for comparison, we select from the literature a few well known examples of very relaxed clusters spanning a similar z range ($0.2 \lesssim z \lesssim 0.3$), characterized by high T_X , and sampled by SDSS. From the relaxed clusters listed by Allen et al. (2004) we select² Abell 383, Abell 963, and Abell 1835 (hereafter A383, A963, A1835). These clusters are all classified as cool core clusters according to Baldi et al. (2007). This agrees with that observations suggest that cool cores are destroyed by cluster mergers and cool core clusters are in the final phase of cluster relaxation (see e.g., Allen et al. 2001; Buote 2002; Sanderson et al. 2006). Among the cool core clusters listed by Baldi et al. (2007) we considered other two cool core clusters to complete our comparison sample: Abell 2261 (hereafter A2261) and ZwCl 1021.0+0426 (hereafter and better known as ZwCl3146).

To avoid the inherent bias that has plagued numerous studies (see the section above), the cluster LFs will be compared based on scaling relative to the dynamical radius, R_{200} . As an estimate of R_{200} , we use R_{vir} definition by Girardi & Mezzetti (2001), Eq. 1 with the scaling of $H(z)$,

$$R_{200} = 0.17 \times \sigma_v / (\text{km s}^{-1}) / H(z) h_{70}^{-1} \text{Mpc}, \quad (1)$$

where σ_v is the LOS velocity dispersion. The same result was obtained by Carlberg et al. (1997, see their Eq. 8 for R_{200}) using a different, more theoretical, approach. Biviano et al. (2006) obtained a 10% smaller estimate of R_{200} , $R_v = 0.15 \times \sigma_v / (\text{km s}^{-1}) / H(z) h_{70}^{-1} \text{Mpc}$ on the base of N-body simulations. We also consider internal and external regions, i.e. $R < 0.5R_{200}$ and $0.5R_{200} < R < R_{200}$, respectively. The centers for relaxed clusters are taken from X-ray studies, while those for DARC clusters are those used in our previous papers. Note that, due to the unrelaxed state of DARC clusters, the choice of the cluster center is not obvious since gas and galaxy spatial distributions are generally different. For A697, A773 and A2219 clusters we used the position of the brightest dominant galaxy, very close to the X-ray centroid (or X-ray main peak), while for A959 and A1240 we use X-ray centroid. However, in these two cases, X-ray centroid is located in between the two brightest dominant galaxies. A radius of $0.5R_{200}$ is sufficient to contain the cores of galaxy subclusters, the most critical case being the bimodal cluster A1240, strongly elongated in the plane of the sky.

As for the mass estimate, in a relaxed cluster, one can use the measured global value of velocity dispersion, $\sigma_{v,\text{tot}}$ to determine R_{200} and then M_{200} within R_{200} . The estimation of mass is based on the virial theorem and, in particular, we follow the prescriptions of Girardi et al. (1998; see also Girardi & Mezzetti 2001). We prompt to the original papers for the details, but, in practice, one can use:

$$M_{200} = A \times [\sigma_v / (10^3 \text{km s})]^3 \times h_{70}^{-1} 10^{15} M_\odot, \quad (2)$$

where $A \sim 1.4$ (here median $A = 1.416$). Thus both our estimates of R_{200} and M_{200} depend on the estimate of the observable value of σ_v . However, they do not are mutually consistent according to the definition: $M_{200} = 200 \times \rho_{\text{crit}} \times 4/3 \times \pi \times R_{200}^3$, where ρ_{crit} is the critical density of the Universe at the cluster redshift. Rather, according to the definition, they correspond to R_{194} and M_{194} .

² Note that we exclude Abell 611 due to its unrelaxed appearance in the SDSS image.

As for the relaxed clusters, we estimate σ_v from the observed T_X assuming the equipartition of energy density between ICM and galaxies, i.e. $\beta_{\text{spec}} = 1$, where $\beta_{\text{spec}} = \sigma_v^2 / (kT / \mu m_p)$ with $\mu = 0.58$ the mean molecular weight and m_p the proton mass. This assumption is particularly appropriate for massive clusters (e.g., Girardi et al. 1996, 1998). R_{200} and M_{200} are thus recovered with the above equations.

For each relaxed cluster, Table 2 lists the main properties: the cluster center (Col. 2); the cluster redshift, z (Col. 3); the X-ray temperature, T_X (Col. 4); the estimated value of σ_v from T_X (Col. 5); the values of R_{200} and M_{200} (Cols. 6 and 7); useful references (Col. 8).

As for the DARC clusters we have to adopt a more complex procedure. During a cluster merger, the global value of velocity dispersion, $\sigma_{v,\text{tot}}$, might strongly vary and not be a very good indicators of the real cluster potential (e.g., Pinkney et al. 1996) and the same problem could afflict T_X (e.g., Ricker & Sarazin 2001; Mastropietro & Burkert 2008). As discussed in our papers for the five DARC clusters, we have detected the main subclusters and obtain an estimate of their individual velocity dispersion, $\sigma_{v,\text{subs}}$. Thus, an alternative, likely more reliable value of the mass M_{200} of the cluster, can then be obtained by adding the masses of all subclusters. Then, inverting the above scaling relation eq. 2, we can obtain a value of the velocity dispersion, σ_v , which should be a better indicator of the potential. The use of eq. 1 leads to the estimate of R_{200} .

For each DARC cluster, Table 1 lists the main properties: the cluster center (Col. 2); the cluster redshift, z (Col. 3); the X-ray temperature, T_X (Col. 4); the global observed value of velocity dispersion, $\sigma_{v,\text{obs}}$ (Col. 5); the (rounded) values of velocity dispersions for subclusters $\sigma_{v,\text{subs}}$ (Col. 6); the estimated value of mass from the addition of subclusters, M_{200} (Col. 7); the corresponding values of σ_v and R_{200} (Cols. 8 and 9). The values of the cluster center, z , T_X , $\sigma_{v,\text{tot}}$, and $\sigma_{v,\text{subs}}$ can be obtained from the listed references. In particular, the notes list the source for the values of $\sigma_{v,\text{subs}}$, here rounded. Other values are homogeneously computed in this study.

3. Magnitude data and background contamination

The magnitude data (r' , i') are taken from SDSS (Data Release 7). We retrieve *model mag* values. For each cluster, we create a galaxy “cluster galaxy sample” by selecting the galaxies in an area centered on the cluster center listed in Tables 2 and 1 and within the respective radius R_{200} . We verify that the whole cluster area is covered by SDSS data by visual inspection.

For each cluster, we also consider a galaxy sample selecting galaxies in one square degree field at 1.5 degree toward the west of each cluster obtaining ten individual field samples. Together these samples, for a total area of ten square degrees, forms the “field galaxy sample” and are used to estimate the field galaxy contamination. Fig. 1 shows the field counts for r' and i' magnitudes, and the logarithmic function fit. This fit represents the count-magnitude relation expected for a homogeneous galaxy distribution in a universe with Euclidean geometry. We obtain the relations $\log(N_r) = 0.455(\pm 0.043)r' - (6.17 \pm 0.59) 0.5 \text{mag}^{-1} \text{deg}^{-2}$ for $15 < r' < 22$ and $\log(N_i) = 0.451(\pm 0.046)i' - (5.70 \pm 0.58) 0.5 \text{mag}^{-1} \text{deg}^{-2}$ for $15 < i' < 21.5$. We used these fits with two purposes: i) to estimate the completeness of our sample; ii) to subtract field galaxy contamination in each cluster.

By comparison with the logarithmic fits, the completeness magnitude can be derived. So, we estimate the photometric sample is complete down to the magnitude counts are lower than

Table 1. Unrelaxed clusters (DARC sample).

Name	α, δ (J2000)	z	T_X keV	$\sigma_{v,tot}$ kms $^{-1}$	$\sigma_{v,subs}$ (kms $^{-1}$)	M_{200} 10 $^{15} M_\odot$	σ_v (kms $^{-1}$)	R_{200} Mpc
A697 ^a	08 42 57.55, +36 21 59.9	0.2815	10.2	1334 $^{+114}_{-95}$	200, 600, 400	0.40	660	1.39
A773 ^b	09 17 53.26, +51 43 36.5	0.2197	7.8	1394 $^{+84}_{-68}$	950, 500	1.39	994	2.16
A959 ^c	10 17 35.04, +59 33 27.7	0.2883	7.0	1170 $^{+83}_{-73}$	600, 700	0.76	824	1.73
A1240 ^d	11 23 37.60, +43 05 51.0	0.1948	6.0	870 $^{+91}_{-79}$	700, 1000	1.93	1103	2.43
A2219 ^e	16 40 19.87, +46 42 41.3	0.2254	10.3	1438 $^{+109}_{-86}$	1000	1.41	1000	2.17

^a Ref.: Girardi et al. 2006; $\sigma_{v,subs}$ from KMM4g1-2-4 in Table 4.

^b Ref.: Barrena et al. 2007; $\sigma_{v,subs}$ from the main and secondary subclusters in Sect. 5.

^c Ref.: Boschin et al. 2008; $\sigma_{v,subs}$ from the averages of KMM1 and V1, and of KMM2 and V2 in Table 2. Here we not consider the subclump V3(=KMM3=DS-NE) also detected in X-ray and thus likely in a premerging phase and not responsible of the ongoing merger.

^d Ref.: Barrena et al. 2009; $\sigma_{v,subs}$ from A1240N and A1240S in Table 2.

^e Ref.: Boschin et al. 2004; $\sigma_{v,subs}$ from NW in Table 2. The separation of suclumps is not obvious. Here, since the primary subclump lies at the SE of the cluster center (see also the more recent paper Million & Allen 2009), we consider the value of σ_v of NW sector, where the main cluster is likely free from the subclump.

Table 2. Relaxed cluster (Comparison sample).

Name	α, δ (J2000)	z	T_X keV	σ_v (kms $^{-1}$)	R_{200} Mpc	M_{200} 10 $^{15} M_\odot$	Refs. ^a
A383	02 48 03.50, -03 31 45.0	0.188	3.9	802	1.78	0.74	Allen et al. 2004, Maughan et al. 2008
A963	10 17 01.20, +39 01 44.4	0.206	6.0	995	2.18	1.41	Allen et al. 2004, Baldi et al. 2007
A1835	14 01 02.40, +02 52 55.2	0.252	8.1	1156	2.47	2.15	Allen et al. 2004, Baldi et al. 2007
A2261	17 22 27.60, +32 07 57.2	0.224	7.2	1090	2.36	1.83	Baldi et al. 2007, Maughan et al. 2008
ZwCl13146	10 23 39.60, +04 11 24.0	0.291	8.6	1191	2.49	2.31	Baldi et al. 2007, Baldi et al. 2007

^a References for z and T_X are listed in the first and second position, respectively. Cluster centers are taken from Ebeling et al. 1996 or Ebeling et al. 1998.

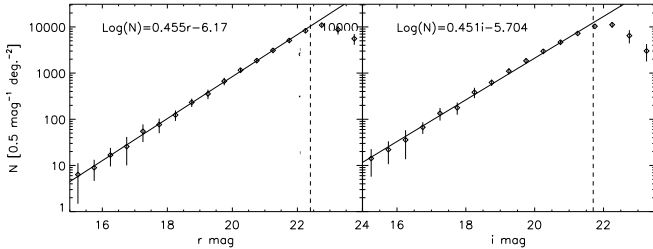


Fig. 1. Values of r' - and i' -band counts for the 10 square degrees considered as the field galaxy sample. The solid line indicates the logarithmic function fit to the histograms. The dashed line indicates the completeness magnitudes.

5% of the fit. Therefore, we consider the r' - and i' -band photometry complete down to $r' = 22.4$ and $i' = 21.4$, respectively. We find that these values are in very good agreement with those reported by the Sloan Digital Sky Survey DR7 (see <http://www.sdss.org/dr7/>).

Two different approaches to the statistical subtraction of the galaxy foreground/background are discussed in the literature: several studies have examined the effect on the derived cluster LF using a global galaxy field correction versus one measured locally for each cluster. For instance, Popesso et al. (2004) has shown, for a study of about 100 clusters based on SDSS data, that there is no significant difference in the measured cluster LF

parameters using either a global or local field subtraction technique. Here we consider the global field correction, subtracting the field counts derived from the logarithmic fits to the cluster counts. Note that the field counts are treated in a different and appropriate way for each cluster before the subtraction.

The magnitudes of each cluster are corrected for the galactic absorption using the Schlegel, Finkbeiner and Davis Galactic reddening maps (Schlegel et al. 1998), derived from IRAS and COBE/DIRBE data.

The possible contamination of distant clusters projected onto the field-of-view of the target cluster can prove to be problematic in the derivation of the LF, in particular at the faint-end. One can use that the spectroscopic studies show that there are essentially no cluster galaxies significantly redward of the red sequence (e.g. Rines & Geller 2008). We minimize the contamination of background clusters using the $r' - i'$ vs. r' colour-magnitude relation which is proved to be the most useful from target clusters are at $0.2 < z < 0.4$ (Lu et al. 2009, their Fig. 6 and Sect. 3.4.1). For each cluster, we fit the red sequence (RS) $r' - i'$ vs. r' for galaxies. We reject galaxies that are 0.15 mag redward of the RS (i.e. ≥ 3 times the average dispersion of the cluster RS). Fig.2 shows an example for the RS in the case of A383. After this background correction, the clusters appear more contrasted with respect to the surrounding field (see Fig. 3 for A383.)

Tab. 3 lists, for each cluster, the slope a and the intercept b , and standard deviations, of the RS $r' - i'$ vs. r' obtained with a linear fit within $0.5 h_{70}^{-1}$ Mpc from the center and for galaxies with $r' < 20.2$ (Col. 2 and 3).

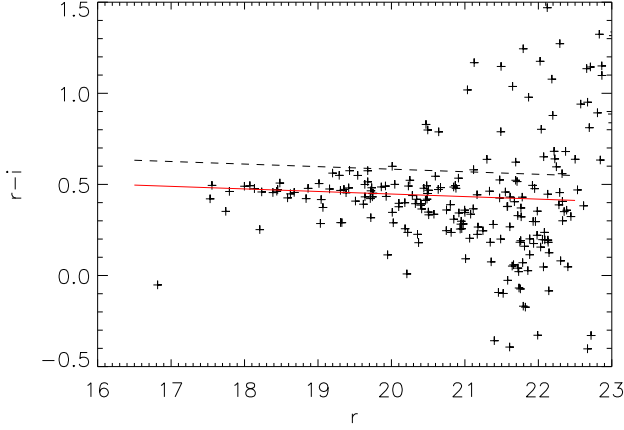


Fig. 2. Color magnitude diagram $r' - i'$ vs. r' considering galaxies within $0.5 h_{70}^{-1}$ Mpc from the center of Abell 383. The RS (red solid line) is fitted using galaxies with $r' < 20.2$. Galaxies with $r' - i' > \text{RS} + 0.15$ (on the dashed line) are considered background galaxies and rejected from the analysis.

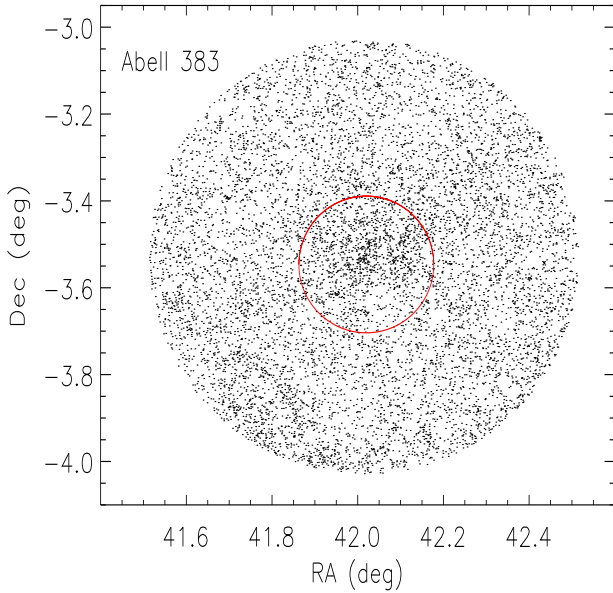


Fig. 3. Galaxies with $r' - i' < \text{RS} + 0.15$ in the region of A383. The red circle indicates R_{200} for this cluster.

Fig. 4 shows the RS parameters vs. cluster redshift. As for the RS slope, there is no correlation with z in the observed range and we estimate a mean value of $\langle a \rangle = -0.017 \pm 0.008$. As for the $r' - i'$ colors at $r' = 17$, as computed from the RS fits, there is no difference in the behaviour of DARC and relaxed clusters: we only observe a marginally higher value for the most distant cluster A697, A959 and ZwCl3146, which is consistent with the k -correction effect on early-type galaxies in the central core of clusters (see Fukugita et al. (1995, tables 3, 6, 7 and 8). Assuming a linear variation of the color with the redshift, we obtain the relation $(r' - i')_{r'=17} = 1.24 * z + 0.23$, with a global dispersion in color of ± 0.02 .

Table 3. Color-magnitude relations (CMR) $r' - i'$ vs. r' linear fits ($az + b$): Red Sequences.

Name	(a, δa)	(b, δb)
A697	-0.0107, 0.014	0.744, 0.041
A773	-0.0213, 0.007	0.861, 0.037
A959	-0.0310, 0.006	1.126, 0.037
A1240	-0.0110, 0.020	0.666, 0.037
A2219	-0.0086, 0.007	0.668, 0.062
A383	-0.0160, 0.001	0.763, 0.047
A963	-0.0422, 0.007	1.216, 0.042
A1835	-0.0004, 0.011	0.501, 0.031
A2261	-0.0091, 0.015	0.653, 0.048
ZwCl3146	-0.0220, 0.003	1.020, 0.050

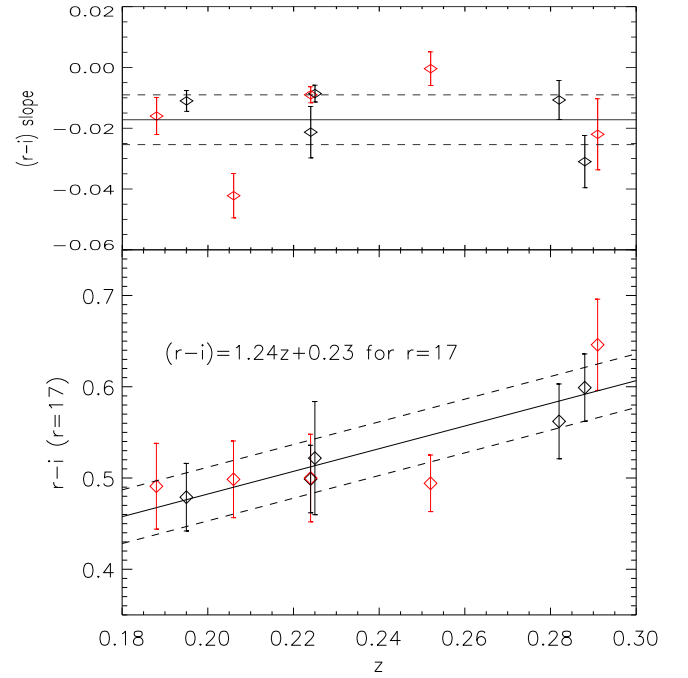


Fig. 4. RS parameters vs. redshift: the $(r' - i')$ vs. r' slope (upper panel) and $(r' - i')$ color at $r' = 17$ (lower panel). Black symbols indicate DARC clusters and red symbols indicate relaxed clusters. The solid line in the upper panel shows the mean value for all ten clusters. The solid line in the lower panel shows the linear fit. The dashed lines show one-sigma uncertainties of the linear fit.

For each cluster, we transform galaxy apparent into absolute magnitudes by applying the relation:

$$M_r = r' - 2.5 - 5 \log(D_L / 1 \text{ Mpc}) - K(z) + E(z), \quad (3)$$

where r' is the apparent magnitude (already corrected for the Galactic absorption, see above), D_L is the luminosity distance; $K(z)$ is the K-correction and $E(z)$ is the evolutionary correction. $K(z)$ and $E(z)$ corrections are applied using a single parametrization based on early-type galaxies, which are dominant in the cluster galaxy population. As for $K(z)$, we use the correction obtained from the Table 2, col. 3 in Roche et al. (2009). As for the evolutionary correction, we use $E(z) = 0.86z$ (Roche et al. 2009). Given that the completeness of magnitude data is

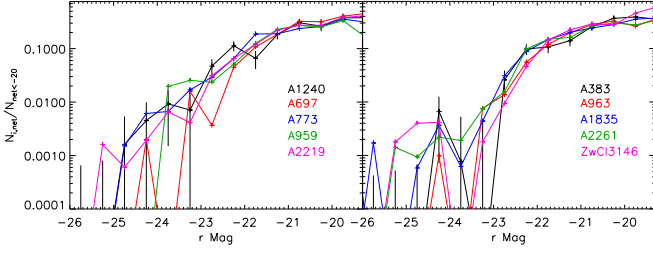


Fig. 5. LFs for DARC clusters (*right panel*) and relaxed clusters (*left panel*) as computed within R_{200} . Error bars are only plotted in the A1240 and A383 LFs for the sake of clarity.

$r' = 22.4$ (Fig. 1) and the most distant cluster of our catalogs is at $z = 0.29$, we expect that the LFs we obtain in the present study are all reliable for absolute magnitude $M_r < -18.6$.

For each cluster, before the field subtraction in the construction of the LF (see below), the field galaxies are treated in the same way of the respective cluster galaxies, i.e. we apply the same correction for the Galactic absorption; the same rejection of very red galaxies; the same transformation in absolute magnitudes.

4. Galaxy populations in DARC and relaxed clusters

4.1. Individual luminosity functions

Fig. 5 shows the individual LFs for DARC and relaxed clusters within R_{200} , where the galaxy counts are computed as $N_i = N_{net,i}/N_{net,<-20}$. $N_{net,i}$ are the net counts, i.e. $N_{net,i} = N_{cluster,i} - N_{field,i}$ where the field counts are opportunely normalized to the cluster area. $N_{net,<-20}$ is the number of net counts for $M_r < -20$ and thus represents the “richness” here used to normalize. The error bars in Fig. 5 are the richness-normalized $\sigma_i = (N_i + N_{b,i} + rms_f^2)^{1/2}$, where the first two terms take into accounts the Poissonian errors of the cluster and background field samples, and the third term measures the field-to-field variation per bin in the background field counts (i.e., the cosmic variance obtained using the ten individual field samples). In order to see possible variations with the radius, we also compute the LFs within $0.5R_{200}$ and R_{200} .

Each LF was fitted to a Schechter function (see Schechter 1976) using the “minuit” procedure (CERN Libraries) to minimize the three values, ϕ (richness), α (slope) and M^* of the Schechter profile. We do not discuss the ϕ parameter since here the counts are already normalized by the “richness” $N_{net,<-20}$ for each cluster. Table 4 shows M^* and α values obtained for each cluster, fitting Schechter function within R_{200} and $0.5R_{200}$.

Fig. 6 shows α vs. M^* values estimated for each cluster within R_{200} : the absence of difference between DARC and relaxed clusters is shown. We obtain the same result for LFs within $0.5R_{200}$ and when comparing R_{200} and $0.5R_{200}$ results.

For the DARC sample we obtain a mean value of $M_{DARC}^* = -21.73 \pm 0.16$ and -21.57 ± 0.16 , considering galaxies within R_{200} and $0.5R_{200}$, respectively. On the other hand, for the relaxed clusters, we derive $M_{rel}^* = -21.58 \pm 0.11$ and -21.48 ± 0.12 . For the slope parameter, we estimate $\alpha_{DARC} = -1.06 \pm 0.09$ and -0.84 ± 0.10 within R_{200} and $0.5R_{200}$, respectively. For the relaxed clusters, we obtain $\alpha_{rel} = -1.00 \pm 0.12$ and -0.84 ± 0.10 . Due to the correlated nature of α and M^* parameters in the fitting procedure, which likely leads to the apparent correlation in Fig. 6, we prefer to compare individual clusters fixing one pa-

Table 4. M_r^* and α values obtained from Schechter fit for the LF.

Name	$R < R_{200}$			$R < 0.5R_{200}$		
	$M_r^*, \Delta M_r^*$	$\alpha, \Delta\alpha$		$M_r^*, \Delta M_r^*$	$\alpha, \Delta\alpha$	
A697	-21.19, 0.30	-0.96, 0.20		-20.95, 0.16	-0.70, 0.21	
A773	-21.84, 0.26	-1.01, 0.13		-21.43, 0.24	-0.61, 0.18	
A959	-21.60, 0.62	-0.96, 0.39		-22.00, 0.94	-0.96, 0.46	
A1240	-22.31, 0.36	-1.28, 0.12		-21.61, 0.37	-0.95, 0.20	
A2219	-21.74, 0.28	-1.09, 0.15		-21.79, 0.08	-0.97, 0.08	
A383	-21.89, 0.25	-1.30, 0.17		-21.92, 0.27	-1.26, 0.21	
A963	-21.31, 0.28	-0.83, 0.19		-20.93, 0.22	-0.27, 0.25	
A1835	-21.78, 0.21	-1.02, 0.15		-22.06, 0.33	-1.13, 0.18	
A2261	-21.56, 0.22	-0.88, 0.16		-21.62, 0.25	-1.01, 0.19	
ZwCl3146	-21.36, 0.26	-0.97, 0.24		-20.89, 0.23	-0.51, 0.29	

rameter and remake the fit. When fixing $\alpha = -1.00$ for the slope parameter for all individual clusters, we find no longer difference (see Table 5). In particular, when fixing the slope, we obtain $M_{DARC}^* = -21.64 \pm 0.06$ and $M_{rel}^* = -21.61 \pm 0.05$ within $R < R_{200}$ and $M_{DARC}^* = -21.82 \pm 0.14$ and $M_{rel}^* = -21.64 \pm 0.06$ within $R < 0.5R_{200}$. From this results, we can conclude that the global LF profile is similar for DARC and relaxed clusters and independent of the sampling radius.

Table 5. M_r^* values obtained from the Schechter fit when fixing $\alpha = -1.00$ for the LF.

Name	$R < R_{200}$	$R < 0.5R_{200}$
	$M_r^*, \Delta M_r^*$	$M_r^*, \Delta M_r^*$
A697	-21.30, 0.12	-21.19, 0.79
A773	-21.85, 0.11	-22.15, 0.12
A959	-21.83, 0.16	-22.25, 0.19
A1240	-21.65, 0.17	-21.69, 0.18
A2219	-21.57, 0.12	-21.81, 0.31
A383	-21.51, 0.14	-21.65, 0.21
A963	-21.54, 0.12	-21.70, 0.13
A1835	-21.75, 0.09	-21.95, 0.14
A2261	-21.72, 0.09	-21.59, 0.11
ZwCl3146	-21.53, 0.13	-21.33, 0.08

The mean LF will be studied in the following subsection, and we will detail possible differences considering blue and red galaxy population in the inner and external regions.

4.2. The composite luminosity functions

For both DARC and relaxed clusters separately, we construct the composite LFs by combining into a single “ensemble” LF, in order to improve the rather poor number statistics for each individual LF. The composite LF is built by averaging, in absolute magnitude bins, the richness-normalized net counts as obtained above for each individual LF. We assume the standard errors on the average.

Fig. 7 shows the composite LFs for DARC and relaxed clusters within R_{200} and $0.5R_{200}$. Table 6 summarizes the M^* and α parameters obtained for the composite LFs. In agreement with the above section, there is no evidence of difference between

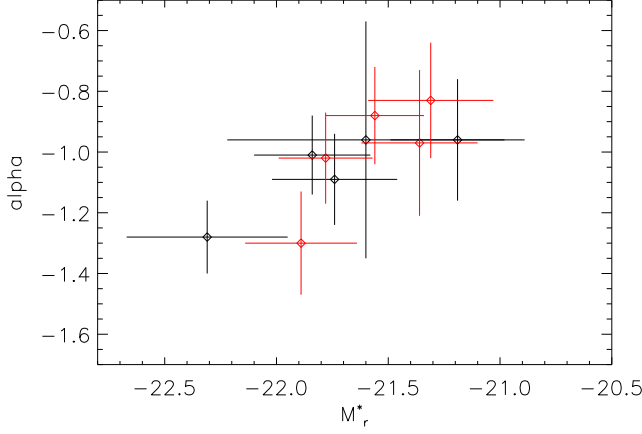


Fig. 6. α vs. M_r^* derived from the Schechter LF fit. Black symbols indicate DARC clusters and red symbols indicate relaxed clusters.

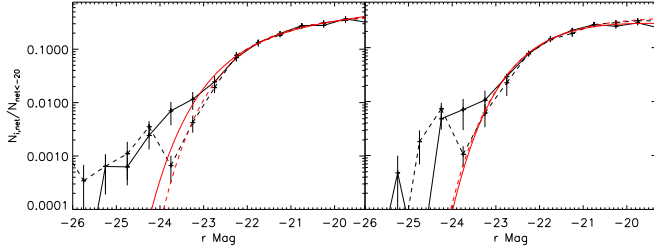


Fig. 7. Composite LFs within R_{200} (left panel) and $0.5R_{200}$ (right panel). Solid lines show the counts for DARC clusters and dashed lines show the counts for the relaxed clusters. The red lines indicate the corresponding Schechter fits.

DARC and relaxed samples and there is no dependence on the sampling radius.

Table 6. M^* and α for the composite LFs.

	$R < R_{200}$		$R < 0.5R_{200}$	
	Whole galaxy population			
Sample	$M^*, \delta M^*$	$\alpha, \Delta\alpha$	$M^*, \delta M^*$	$\alpha, \Delta\alpha$
<i>DARC</i>	-22.00, 0.41	-1.20, 0.17	-21.64, 0.35	-0.86, 0.27
<i>Relaxed</i>	-21.63, 0.24	-1.03, 0.20	-21.74, 0.29	-0.99, 0.21
	Red galaxies			
<i>DARC</i>	-21.62, 0.25	-0.76, 0.22	-21.23, 0.28	-0.47, 0.27
<i>Relaxed</i>	-21.51, 0.28	-0.76, 0.23	-21.50, 0.36	-0.70, 0.30
	Blue galaxies			
<i>DARC</i>	-22.55, 0.27	-2.03, 0.10	-22.98, 0.37	-1.79, 0.24
<i>Relaxed</i>	-21.66, 0.52	-1.44, 0.46	-23.63, 0.53	-2.07, 0.23

Fig. 7 shows as the Schechter functions fit reasonably well the counts for galaxies with $M_r > -22.5$. We obtain ³ $\chi^2 = 0.45$

³ The χ^2 statistic has been calculated considering three degrees of freedom, the normalization coefficient, M^* and the slope.

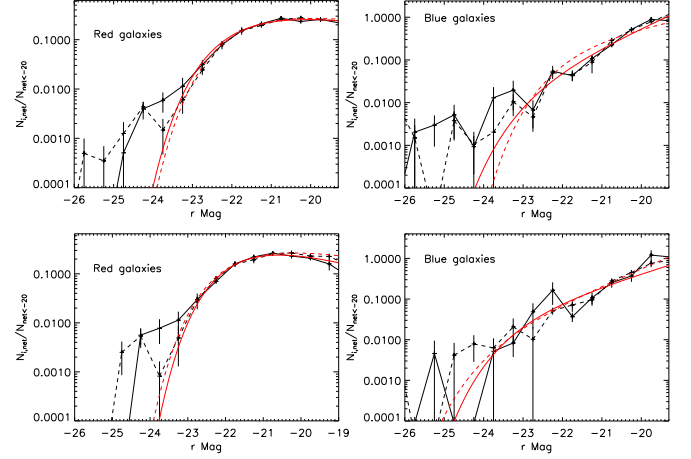


Fig. 8. Upper panels: LFs and Schechter fits for red and blue galaxies computed within R_{200} . Lower panels: the same within $0.5R_{200}$. Solid lines indicate DARC clusters and dashed lines indicate relaxed clusters.

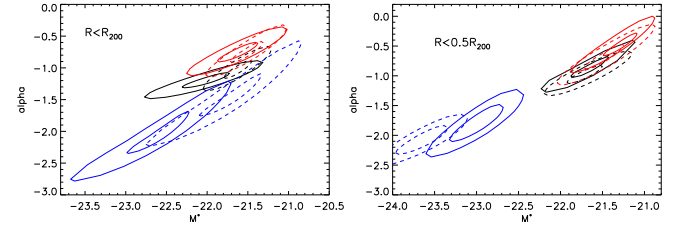


Fig. 9. Error contours at the 1 and 3σ c.l. for the best-fitting LF parameters considering the galaxy population within $R < R_{200}$ (left panel) and $R < 0.5R_{200}$ (right panel). Black, red and blue lines show the composite LF for the whole galaxy sample, red and blue galaxies, respectively. Solid lines indicate DARC clusters and dashed lines indicate relaxed clusters.

for DARC clusters and 0.35 for relaxed clusters (both within R_{200}) and $\chi^2 = 0.33$ for DARC clusters and 0.27 for relaxed clusters (both within $0.5R_{200}$). On the contrary, the bright-end ($M_r < -22.5$) is not well represented by Schechter functions. In any case, we obtain χ^2 values higher than 1.4. Therefore, the contribution of these bright galaxies (hereafter BGs) have to be analyzed separately (see Sect. 5).

4.3. Blue and red LFs

We also estimate LF for red and blue galaxies within R_{200} and $0.5R_{200}$. We select red and blue galaxies from the RS (see above). We assume red galaxies those objects within the RS, that is $RS-0.15 < r' - i' < RS+0.15$, while blue galaxies were selected as $r' - i' < RS-0.15$. Results are presented in Fig. 8 and summarized in Table 6.

When considering the whole galaxy population, no differences are found between DARC and relaxed clusters within R_{200} or inside the core of the clusters, within $0.5R_{200}$. The differences in M^* and α are not significant and within 3σ errors (see Fig. 9). The same is also true for the red galaxy population. We only note a marginal difference in the LF parameters of blue galaxies, in particular in the core of the clusters, inside $0.5R_{200}$.

To check the significance of these differences, we fit the Schechter profiles to the composite LFs fixing the slope pa-

parameter. Table 7 lists the results obtained. Again, we confirm no differences between DARC and relaxed LFs. As above, we only find small differences for the blue galaxy population within $0.5R_{200}$. However, this difference should be taken with care since the blue galaxy population is very poor in the internal regions of the clusters thus limiting number of considered counts.

Table 7. M^* for the composite LFs (at fixed α).

	$R < R_{200}$	$R < 0.5R_{200}$
Whole galaxy population ($\alpha = -1.00$)		
Sample	$M^*, \delta M^*$	$M^*, \delta M^*$
DARC	-21.61, 0.07	-21.83, 0.06
Relaxed	-21.59, 0.05	-21.75, 0.06
Red galaxies ($\alpha = -0.70$)		
DARC	-21.54, 0.07	-21.52, 0.05
Relaxed	-21.44, 0.05	-21.48, 0.06
Blue galaxies ($\alpha = -2.00$)		
DARC	-22.74, 0.52	-23.18, 0.11
Relaxed	-22.38, 0.11	-23.56, 0.06

4.4. Butcher-Oemler effect

The window opened by the redshift dependence of the galaxy properties has been used to set constraints on the time-scales of the processes of galaxy evolution (Butcher & Oemler, 1978, 1984; Stanford et al. 1998). In this context, the observational evidence of the environmental effect is still uncertain. In order to clarify whether merging processes in clusters can enhance the star formation in the galaxy populations, we compare the fraction of blue galaxies, f_B , in DARC and relaxed clusters. So we quantify the Butcher-Oemler effect (Butcher & Oemler, 1978, 1984) in two homogeneous cluster samples with similar velocity dispersions and masses.

Studies of Andreon et al. (2006) show that the radial dependence of the blue fraction is quite shallow, and it smoothly and monotonically increases from the center of the cluster to the field (see Fig. 10 in Andreon et al. 2006). However, the contamination contribution of field galaxies is lower in the inner regions. For this reason, we estimate f_B within $0.5R_{200}$.

Fig. 10 shows as f_B increases towards high redshifts being at the 95% c.l. according to the Kendall statistics. A linear fit gives $f_B(z) = 1.18(\pm 0.07)z - 0.07(\pm 0.06)$ (see also Sect. 7 for further discussions). We find no significant difference between f_B of DARC and relaxed clusters.

5. The bright end of the LF

Here we define bright galaxies (BGs) those galaxies with $M_{r'} < -22.5$ and analyze whether DARC and relaxed clusters differ for their BGs, in counts or luminosity.

5.1. Counting BGs

Fig. 11 shows the number of BGs for each cluster $N_{BG} = N_{r' < -22.5} / N_{r' < -20} \langle N \rangle$, where $N_{r' < -22.5}$ is the number of galaxies brighter than $M_{r'} < -22.5$ (normalized to the cluster richness, see the above Sect. 4) and $\langle N \rangle = \langle N_{r' < -20} \rangle$ is the

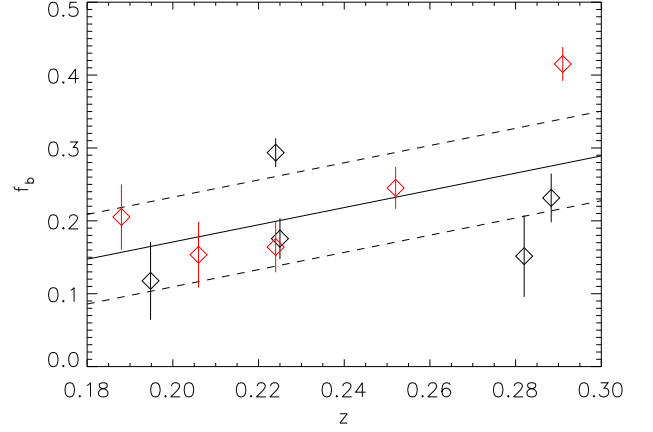


Fig. 10. Fraction of blue galaxies within $0.5R_{200}$ for DARC (black symbols) and relaxed clusters (red symbols). The solid line describes the linear fit of this relation. The dashed lines show one-sigma uncertainties of the linear fit.

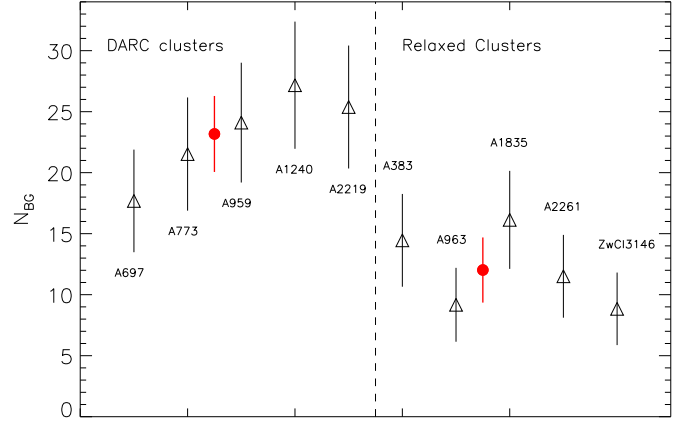


Fig. 11. Number of bright galaxies within R_{200} . Vertical dashed lines separate DARC and relaxed cluster samples. Labels indicate individual clusters. The red points represent the mean value computed for each cluster sample separately.

mean richness as computed on all clusters. Here we multiply for the mean richness to obtain more realistic BG counts. Error bars are assumed to be the Poissonian errors. The figure shows as the BG counts are higher in DARC clusters than in relaxed clusters. Considering the cluster regions within R_{200} , the mean values for both samples separately are $N_{BG,DARC} = 23.1 \pm 3.1$ and $N_{BG,rel} = 12.0 \pm 2.7$ for DARC and relaxed clusters. Therefore, DARC clusters contain a factor two more BGs than relaxed clusters and the difference is significant at the 2.7σ c.l..

We also study the spatial distribution of BG galaxies. We compute BG counts in two separate regions, $R < 0.5R_{200}$ and $0.5R_{200} < R < R_{200}$ (see Fig. 12). For the inner cluster region, $R < 0.5R_{200}$, we obtain $N_{BG,DARC} = 10.9 \pm 2.7$ and $N_{BG,rel} = 7.2 \pm 2.4$. For the outer cluster region, $0.5R_{200} < R < R_{200}$, we obtain $N_{BG,DARC} = 20.2 \pm 2.5$ and $N_{BG,rel} = 8.3 \pm 2.1$. Thus the difference in BG counts is restricted to the outer region, where is significant at 3.6σ c.l..

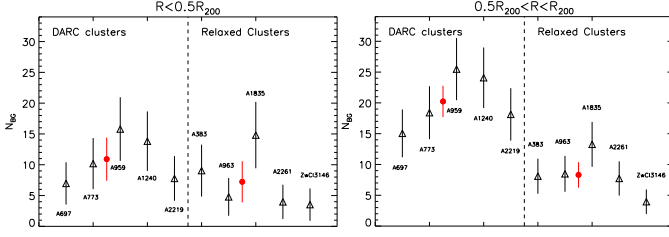


Fig. 12. BG counts in the inner region, $R < 0.5R_{200}$ (left panel) and in the outer region, $0.5R_{200} < R < R_{200}$ (right panel). Symbols are the same as in Fig. 11.

We correlate N_{BG} with the redshift and the mass of the cluster. We do not observe any clear relation in both $N_{\text{BG}} - z$ and $N_{\text{BG}} - M_{200}$ relations.

Our above results are based on photometric BG counts opportunely corrected with the average field counts (see Sect. 4.1). Due to the poor number statistic of BGs in the individual clusters, we also use another approach to check the above results. We also resort to the SDSS spectroscopic survey since redshift data can provide the correct cluster membership. Unfortunately, SDSS survey is not spectroscopically complete. Indeed, within the cluster regions of our sample, SDSS DR8 provide redshifts z for 60% of galaxies having $M_r < -22.5$. Thus, we cannot assess the cluster membership for all BGs. Here we consider a mixed approach: we counts BGs in the photometric sample and then weight these numbers on the base of the spectroscopic information.

As for photometric data, Table 8 lists the mean number of BGs for DARC and relaxed cluster (Cols. 2 and 3); the respective difference and ratio between N_{BG} in DARC and relaxed clusters (Cols. 4 and 5). These values confirm that the strong difference between DARC and relaxed clusters are due to the outer cluster region, while nothing can be said about the inner region due to the poor number statistics. Note that here we do not normalize with the respective cluster richness as in the above section: the net effect would be of slightly reducing the observed difference between DARC and relaxed clusters. Therefore, the results of this section should be looked at as being very conservative.

We use the spectroscopic information to weight the above ratios. We consider galaxy members those galaxies with a difference of $\delta z = 0.01$ ($\delta z = 0.007$) from the cluster redshift, i.e. $\delta cz \sim 3000 \text{ km s}^{-1}$ ($\sim 2000 \text{ km s}^{-1}$) from the mean cluster velocity. Table 8 lists the number of cluster BGs over the number of all BGs having redshift, N_{mem}/N_z , for DARC and relaxed cluster (Cols. 6 and 7), and the values of the ratios DARC/relaxed now weighted with the respective N_{mem}/N_z , i.e. $\text{WRatio}(\text{DARC}/\text{rel}) = \text{Ratio}(\text{DARC}/\text{rel}) \times [N_{\text{mem}}/N_z(\text{DARC})] \times [N_{\text{mem}}/N_z(\text{rel})]^{-1}$ (Col. 8). When comparing the values of “WRatio” with those of above “Ratio” we see that the result of DARC clusters being richer in BGs than relaxed cluster within $0.5R_{200}$ is confirmed.

6. BGs Luminosity

We investigate whether the contribution in luminosity of BGs is different between DARC and relaxed clusters. We compute the “global” luminosity for $M_r < -20$ using the counts of Sect. 4, i.e.:

$$L_{\text{global}} = \sum_i^N N_i(m) l_i(m), \quad (4)$$

where the sum is performed over all the N magnitude bins with galaxy number $N_i(m)$ and mean luminosity $l_i(m)$. The transformation from absolute magnitudes to absolute luminosity in units of solar luminosities is performed using the solar magnitude $M_{r\odot} = 4.62$. The luminosity associated to BGs, L_{BG} , is computed in the same way out to $M_r < -22.5$. Table 9 lists the luminosities for each cluster. Values within parenthesis are errors estimated at 1σ c.l..

Table 9. Luminosity content of BGs.

Name	L_{global} ($10^{12} L_{\odot}$)	L_{BG} ($10^{12} L_{\odot}$)
A697	4.38(0.24)	0.68(0.04)
A773	10.71(2.33)	3.43(0.75)
A959	7.20(2.11)	2.53(0.74)
A1240	16.14(4.74)	10.78(3.17)
A2219	12.08(2.96)	3.32(0.81)
A383	3.03(0.63)	2.90(0.60)
A963	6.29(0.67)	0.78(0.08)
A1835	16.95(2.74)	7.04(1.14)
A2261	12.31(2.52)	2.55(0.53)
ZwCl3146	6.95(3.52)	1.74(0.09)

Note that L_{BG} represents a non-negligible fraction of the global luminosity for $M_r < -20$ and the ten clusters span over a wide range of luminosities. We observe two dramatic cases, these are A1240 in the DARC cluster sample and A383 in the relaxed sample, where the luminosity fraction associated to the BGs, $f_{\text{L,BG}}$, are about 67% and 96% of the total luminosity, respectively. Considering the whole samples, we find that the mean luminosity fractions of BGs are $f_{\text{L,BG,DARC}} = 0.35 \pm 0.19$ and $f_{\text{L,BG,rel}} = 0.39 \pm 0.33$ for DARC and relaxed clusters. If we do not consider the two extreme cases of A1240 and A383, we find $f_{\text{L,BG,DARC}} = 0.27 \pm 0.09$ and $f_{\text{L,BG,rel}} = 0.25 \pm 0.13$. From these values, we conclude that DARC and relaxed clusters do not significantly differ for the luminosity content associated to their BGs.

7. Discussion & conclusions

We compare five unrelaxed clusters (DARC sample) with relaxed clusters. As far as possible we have potential biases under control. The relaxed clusters are similar to unrelaxed clusters for their redshift range, X-ray temperature, and mass (see Tables 1 and 2). Moreover, we always work within physical rather than fixed radii.

We find that very unrelaxed are comparable to relaxed clusters for the statistical properties, i.e. the parameters of the LF and the relative behaviour between red and blue galaxies. In particular, we agree with a series of previous results.

We compare M^* and α parameters of the composite Schechter luminosity functions with results obtained by Popesso et al. (2006). Transforming their M^* estimates (see their Tables 1 and 2) to our cosmology, applying the factor $5 \log(h_{70})$, we obtain values in perfect agreement.

In addition, in agreement with Popesso et al. (2006, their Fig. 10) and de Filippis et al. (2011, their Fig. 11) the LF profile does not depend on the considered cluster region within $M_r < -19$.

Table 8. BGs in photometric samples weighted with spectroscopic samples.

	from photometric survey				from spectroscopic survey		photo + spec
	$N_{\text{BG,DARC}}$	$N_{\text{BG,rel}}$	Diff.	Ratio	$N_{\text{mem}}/N_z(\text{DARC})^a$	$N_{\text{mem}}/N_z(\text{rel})^a$	WRatio ^a
$R < R_{200}$	65	45	20 ± 10	1.4	10/41(8/41)	8/25(6/25)	1.1(0.9)
$R < 0.5R_{200}$	13	16	3 ± 6	0.8	4/13(4/13)	4/8(4/8)	0.5(0.5)
$R > 0.5R_{200}$	52	29	23 ± 9	1.8	6/28(4/28)	4/17(2/17)	1.6(2.2)

^a Where member galaxies are those having $\delta z = 0.01$ ($\delta z = 0.007$).

We also find evidence of the variation of the blue fraction of galaxies with redshift. It is very noticeably that we can detect the effect even if our study is limited to a small redshift range. In particular, note that extrapolating our $f_B(z)$ relation to $z=0.35$, we obtain a $f_B(z = 0.35) = 0.34 \pm 0.05$. This estimate well agrees with those obtained by Andreon et al. (2006). They find $f_B(z = 0.35) = 0.33 \pm 0.05$ with clusters located in a redshift range $0.3 - 0.4$. When extrapolating to $z = 0.5$, we obtain $f_B(z = 0.5) \sim 0.5$. This finding is in very good agreement with cosmological galaxy formation models for cluster with similar mass (see Menci et al. 2008, their Fig. 3).

Our new first result is that relaxed clusters contain fewer BGs and these BGs are more concentrated in cluster inner regions. On the contrary, unrelaxed clusters present more BGs and more homogeneously distributed within the whole cluster. The BG richness of DARC clusters is the robust and significant result of Sect.5.

Our result is not in contrast with that of de Propriis et al. (2003) who found similar LF between substructured and non substructured clusters since: i) their study is devoted to LF parameters, for which we find no difference, too; ii) our sample of DARC clusters are likely to be much more far from dynamical equilibrium than their sample of substructured clusters. In fact, DARC clusters are found to be cases of major, very important mergers, in agreement with the rarity of the diffuse radio sources phenomena ($\sim 10\%$ of clusters, Giovannini & Feretti 2002). Moreover, DARC clusters should all be recent mergers since radio emissions are expected to have a short life time, i.e. of the order of a few 10^8 years (e.g., Giovannini & Feretti 2002; Skillman et al. 2010), in agreement with times estimated in a few individual clusters (e.g., Markevitch et al. 2002; Girardi et al. 2008).

Our second, new result is that the luminosity content in BGs is the same in DARC and relaxed clusters. The consequent scenario is that the (more numerous) BGs lying in the outer regions of merging clusters will merge to form (more luminous) BGs in the inner regions of relaxed clusters. This combined formation/evolution of BGs and the parent clusters well agree with the results of Lin & Mohr (2004) who analyzed the correlation between BCG luminosity and parent cluster mass, supporting a recent formation of the brightest galaxies in the context of the hierarchical scenario.

We plan to extend our study to a larger sample of DARC clusters, by examining their dynamics to compute more reliable mass estimates. Another possible extension of this work is looking at deeper magnitudes thus to investigate possible effects on the faint end of the galaxy LF connected with the cluster evolution.

Acknowledgements. We are in debt with Andrea Biviano for his useful comments on this work. We also thanks for the creation and distribution of the SDSS Archive, provided by the Alfred P. Sloan Foundation and other Participating

Institutions. The SDSS Web site is <http://www.sdss.org/>. This work has been funded by the Spanish Ministry of Science and Innovation (MICINN) under the collaboration grants AYA2010-21887-C04-04 and AYA2010-21322-C03-02. MG acknowledges financial support from PRIN-INAF-2010.

References

- Allen, S. W., Ettori, S., & Fabian, A. C. 2001, MNRAS, 324, 877
 Allen, S. W., Schmidt, R. W., Ebeling, H., Fabian, A. C., van Speybroeck, L. 2004, MNRAS, 353, 457
 Andreon, S., Quintana, H., Tajer, M., Galaz, G., Surdej, J. 2006, MNRAS, 365, 915
 Ascaso, B., Aguerri, J. A. L., Varela, J., et al. 2011, ApJ, 726, 69
 Baldi, A., Ettori, S., Tozzi, P. & Borgani, S. 2007, ApJ, 666, 835
 Barkhouse, W. A., Yee, H.K.C., & López-Cruz, O. 2007, ApJ, 671, 1471
 Barrena, R., Boschini, W., Girardi, M., & Spolaor, M. 2007a, A&A, 467, 37
 Barrena, R., Girardi, M., Boschini, & Dasí, M. 2009, A&A, 503, 357
 Bautz, L. P., & Morgan, W. W. 1970, ApJ, 162, 149
 Binggeli, B., Sandage, A., Tamman, G. A. 1988, ARA&A, 26, 509
 Biviano, A., Murante, G., Borgani, S., Diaferio, A., Dolag, K., & Girardi, M. 2006, A&A, 456, 23
 Boschini, W., Barrena, R., Girardi, M., & Spolaor, M. 2008, A&A, 487, 33
 Boschini, W., Girardi, M., Barrena, R., et al. 2004, A&A, 416, 839
 Butcher, H., & Oemler, A. 1978, ApJ, 219, 18
 Brunetti, G., Cassano, R., Dolag, K., & Setti, G. 2009, A&A, 507, 661
 Buote, D. A. 2002, in "Merging Processes in Galaxy Clusters", eds. L. Feretti, I. M. Gioia, & G. Giovannini (The Netherlands, Kluwer Ac. Pub.): Optical Analysis of Cluster Mergers
 Butcher, H., & Oemler, A. 1984, ApJ, 285, 426
 Carlberg, R. G., Yee, H. K. C., Ellingson, E., et al. 1996, ApJ, 462, 32
 Carlberg, R. G., Yee, H. K. C., & Ellingson, E. 1997, ApJ, 478, 462
 Cassano, R., Ettori, S., Giacintucci, S., et al. 2010, ApJ, 721, 82
 de Filippis, E., Paolillo, M., Longo, G., et al. 2011, MNRAS, 414, 277
 de Lucia, G. & Blaizot, J. 2007, MNRAS, 375, 2
 de Propriis, R., Pritchet, C. J., Harris, W. E., McClure, R. D. 1995, ApJ, 450, 534
 de Propriis, R., et al. 2003, MNRAS, 342, 725
 Dressler, A. 1978, ApJ, 223, 765
 Dressler, A. 1980, ApJ, 236, 351
 Driver, S. P., Couch, W. J., & Philipps, S. 1998, MNRAS, 301, 369
 Dubinski, J. 1998, ApJ, 502, 141
 Durret, F., Laganá, T. F., & Haider, M. 2011, A&A, 529, A38
 Ebeling, H., Voges, W., Böhringer, H., et al. 1996, MNRAS, 281, 799
 Ebeling, H., Edge, A. C., Böhringer, H., et al. 1998, MNRAS, 301, 881
 Ensslin, T. A., Biermann, P. L., Klein, U., & Kohle, S. 1998, A&A, 332, 395
 Feretti, L., Gioia I. M., and Giovannini G. eds., 2002b, Astrophysics and Space Science Library, vol. 272, "Merging Processes in Galaxy Clusters", Kluwer Academic Publisher, The Netherlands
 Feretti, L. 2006, Proceedings of the XLIIth Rencontres de Moriond, XXVIth Astrophysics Moriond Meeting: "From dark halos to light", L.Tresse, S. Maurogordato and J. Tran Thanh Van, Eds, e-print astro-ph/0612185
 Feretti, L. 2008, Mem. SAIt, 79, 176
 Fukugita, M., Shimasaku, K., & Ichikawa, T. 1995, PASP, 107, 945
 Gilbank, D. G., Yee, H. K. C., Ellingson, E., et al. 2008, ApJ, 673, 742
 Giovannini, G., & Feretti, L. 2002, in "Merging Processes in Galaxy Clusters", eds. L. Feretti, I. M. Gioia, & G. Giovannini (The Netherlands, Kluwer Ac. Pub.): Diffuse Radio Sources and Cluster Mergers
 Girardi, M., Boschini, W., & Barrena, R. 2006, A&A, 455, 45
 Girardi, M., Fadda, D., Giuricin, G. et al. 1996, ApJ, 457, 61
 Girardi, M., Giuricin, G., Mardirossian, F., Mezzetti, M., & Boschini, W. 1998, ApJ, 505, 74
 Girardi, M., & Mezzetti, M. 2001, ApJ, 548, 79

- Girardi, M., Barrena, R., & Boschin, W. 2007, Contribution to “Tracing Cosmic Evolution with Clusters of Galaxies: Six Years Later” conference – <http://www.si.inaf.it/sesto2007/contributions/Girardi.pdf>
- Girardi, M., Barrena, R., Boschin, W., & Ellingson, E. 2008, *A&A*, 491, 379
- Hilton, M., et al. 2005, *MNRAS*, 363, 661
- Iglesias-Páramo, J., Boselli, A., Gavazzi, G., Cortese, L., & Vílchez, J. M. 2003, *A&A*, 397, 421
- Keshet, U., & Loeb, A. 2010, *ApJ*, 722, 737
- Keshet, U. 2011, *MNRAS*, submitted (preprint arXiv:1011.0729)
- Lin, Y.-T., & Mohr, J. J. 2004, *ApJ*, 617, 879
- López-Cruz, O., Yee, H.K.C., Brown, J. P., Jones, C., Forman, W. 1997, *ApJ*, 475, 97
- Lu, T., Gilbank, D. G., Balogh, M. L., & Bognat, A. 2009, *MNRAS*, 399, 1858
- Markevitch, M., Gonzalez, A. H., David, L., et al. 2002, *ApJ*, 567, 27
- Mastropietro, C., & Burkert, A. 2008, *MNRAS*, 389, 967
- Maughan, B. J., Jones, C., Forman, W., & van Speybroeck, L. 2008, *ApJS*, 174, 117
- Menci, N., Rosati, P., Gobat, R. 2008 *ApJ*, 685, 863
- Mercurio, A., Massarotti, M., Merluzzi, P., La Barbera, F. & Busarello, G. 2003, *A&A*, 408, 57
- Merritt, D. 1985, *ApJ*, 289, 18
- Million, E. T., Allen, S. W. 2009, *MNRAS*, 399, 1307
- Ostriker, J. P., & Tremaine, S. D. 1975, *ApJ*, 202, 113
- Pinkney, J., Roettiger, K., Burns, J. O. & Bird, C. M. 1996, *ApJS*, 104, 1
- Poggianti, B. M. 2005, Available online at <http://pos.sissa.it> (Proceedings of Science) - eds. R.J. Dettmar, U. Klein, P. Salucci - Invited lecture at the Bochum/Bonn Graduate Research School “Baryons in Dark Matter Halos” (Novigrad, Oct 2004)
- Popesso, P., Biviano, A., Böhringer, H., & Romaniello, M. 2006, *A&A*, 445, 29
- Popesso, P., Böhringer, H., Brinkmann, J., Voges, W., & York, D. G. 2004, *A&A*, 423, 449
- Ramella, M., Biviano, A., Pisani, A., et al. 2007, *A&A*, 470, 39
- Ricker, P. M., & Sarazin, C. L. 2001, *ApJ*, 561, 621
- Rines, K., Geller, M. J. 2008, *AJ*, 135, 1837
- Roche, N., Bernardi, M., Hyde, J. 2009, *MNRAS*, 398, 1549
- Rudnick, G., Von der Linden, A., Pelló, R., et al. 2009, *ApJ*, 700, 1559
- Ruszkowski, M., & Springel, V. 2009, *ApJ*, 696, 1094
- Sanderson, A. J. R., Ponman, T. J., & O’Sullivan, E. 2006, *MNRAS*, 372, 1496
- Schechter, P. 1976, *ApJ*, 203, 297
- Schlegel, D.J., Finkbeiner, D.P., & Davis, M. 1998, *ApJ*, 500, 525
- Skillman, S. W., Hallman, E. J., O’Shea, B. W., et al. 2011, *ApJ*, 735, 96
- Stanford, S. A., Eisenhardt, P. R., Dickinson, M. 1998, *ApJ*, 492, 461
- Stott, J.P., Collins, C.A., Sahlén, M., et al. 2010, *ApJ*, 718, 23
- Tribble, P. C. 1993, *MNRAS*, 261, 57
- Valotto, C. A., Nicotra, M. A., Muriel, H., & Lambas, D. G. 1997, 479, 90
- Valotto, C. A., Muriel, H., Moore, B. & Lambas, D. G. 2004, 601, 67
- Whitmore, B. C., & Gilmore, D. M. 1991, *ApJ*, 367, 64